Initial Events during the Passivation of Rapidly Dissolving Aluminum Surfaces

Yongsug Tak[a] and Kurt R. Hebert*

Department of Chemical Engineering, Iowa State University, Ames, Iowa 50011

ABSTRACT

The early stages of oxide film passivation of corroding surfaces in aluminum etch tunnels and pits were investigated. Passivation was initiated by step reductions in applied current. A mathematical model for passivation was used to predict experimentally measured potential transients during the first millisecond after the current step. The experimental transients had a characteristic potential undershoot at about 70 μs after the current step; according to the model, the undershoot was directly related to the partial coverage of the corroding surface with an oxide layer. The time and extent of the undershoot were in quantitative agreement with the theoretical predictions, suggesting that the fractional actively dissolving area in the pit at these times is a linear function of potential and adjusts rapidly to changes of the potential. This reconfiguration of the active area occurs at times when the extent of passive film formation is still small. A chemical mechanism for passivation which is consistent with the model is one in which the fractional active area is controlled by the coverage of specifically adsorbed chloride ions. Agreement between experimental and predicted potential transients was also observed at room temperature, where no tunnels are found, but only corrosion pits with irregular shapes.

An understanding of the passivation of dissolving metal surfaces by surface oxide films is important for localized corrosion control and also for control of the shapes of etching microstructures. Depassivation of corroding surfaces is attributed by various authors to factors such as solution acidity, or to salt films and adsorbed layers, the presence of which blocks access of passivating water to the metal.[1] However, observations and models of passivation have generally been concerned primarily with the spatially averaged behavior of the surface, and the role of heterogeneous surface phenomena has not been examined.

The present work is a theoretical and experimental study of passivation within aluminum etch tunnels, which are produced by anodic etching of pure aluminum in aqueous chloride solution at temperatures above 60°C.[2,3] Etch tunnels have widths of about 1 μm and penetrate the metal in <100> crystallographic directions. During the growth of a tunnel, metal dissolution occurs from its end, or tip, surface, at current densities of several A/cm^2, while the tunnel sidewalls are covered with an oxide film which inhibits corrosion. As a result of the linear geometry of tunnels, the corroding tip surface can be readily identified in microscopic observations, so that topographic changes resulting from its passivation can be monitored. Tunnel structures become evident at etching times of a few seconds. For etch times less than 1 s, only cubic crystallographic etch pits are present.

Reduction of the applied current during etching initiates partial passivation of the corroding tip surface.[3] In the preceding paper, Tak, Henderson, and Hebert[4] studied the transient topographic evolution of the tip surface during passivation, using scanning electron microscopy (SEM). Tunnel tips were flat crystallographic surfaces when no current reduction had been applied. When the current had been reduced for periods of tens of milliseconds, a number of recessed patches about 0.1 μm wide were found, which were identified as regions of localized metal dissolution. These patches contained all the applied etching current after the current step. The SEM allowed patches to be observed at times as small as 20 ms after passivation initiated. Similar recessed patches were also found on the surfaces of cubic etch pits, after current step experiments carried out at 100 ms etching time. In the case of these pits, the atomic force microscope (AFM) was used to image the etched surfaces. Separation of actively dissolving and passive surfaces in pits was observed at times as early as 5 ms after passivation began.

In this work, a mathematical model was developed which described the progress of passivation at times of less than 1 ms after its initiation. The concepts of the model are in agreement with the observations about surface topography described above, which were made at times of tens of milliseconds. In particular, the model assumes that the surface being passivated is always heterogeneous, consisting of separated active and passive areas. The predictions of the model were compared to experimental potential transients. Through this comparison, information about the controlling influence of the potential on the initiation of oxide film coverage was obtained. Results are presented for etch tunnels, and also for room temperature pitting, to investigate the general applicability of the model to other types of aluminum corrosion. A chemical mechanism of passivation which is consistent with the model is then discussed.

Experimental

Specimens used in the etching experiments were 99.98% purity aluminum foil (Toyo) which had been manufactured for electrolytic capacitor applications. The foil was placed in a glass holder so that an area of 5.07 cm^2 was exposed to the etching solution. A platinum wire was used as a counterelectrode and was bent into a semicircle and fixed on the holder, giving the same geometric arrangement of electrodes in each experiment. A reference electrode (Ag/AgCl/4*M* KCl) was positioned behind the holder during etching; the measured potential was insensitive to the exact location of the reference electrode. All potentials reported in this paper are referred to this reference electrode. Etching was carried out at 65°C in 1*N* HCl solution which was prepared from reagent grade HCl and deionized water. Prior to etching experiments, specimens were pretreated in 1*N* NaOH solution at room temperature for 20 min, washed with water, and dried in air. Samples etched after this pretreatment were found to contain a uniform tunnel length distribution, and also the extent of passivation was ap-

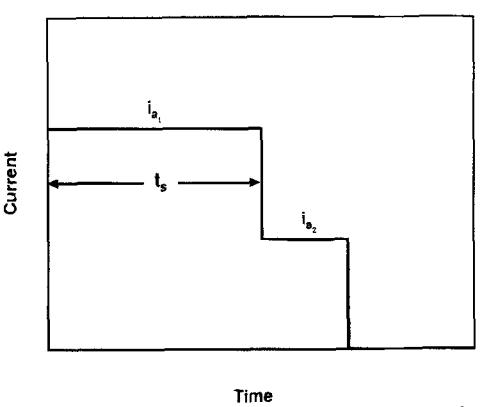

Fig. 1. Applied current waveform for step experiments showing the definitions of symbols used in the model.

* Electrochemical Society Active Member.
[a] Present address: Samsung Electro-Mechanics Co., Suwon, Korea.

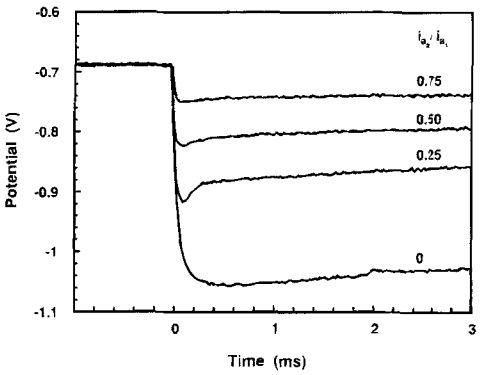

Fig. 2. Portion of potential transients at early times after step reductions of applied current. The parameter is i_{a2}/i_{a1}. Temperature 65°C, etchant 1*N* HCl, base applied current density 40 mA/cm^2, step time 5 s.

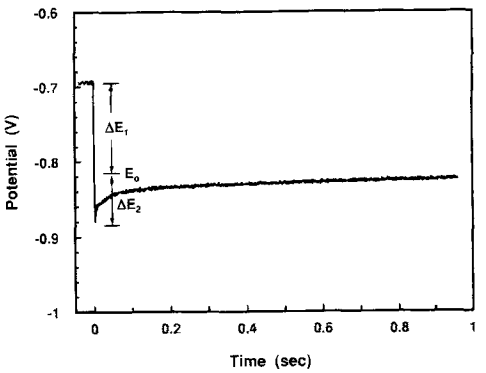

Fig. 3. Potential transient after step reduction in applied current, illustrating the definitions of some symbols. Etching was at 65°C in 1*N* HCl, at a current density of 60 mA/cm^2. i_{a2}/i_{a1} was 0.30.

proximately uniform on each tunnel.[5] The etching current was applied immediately after specimens were immersed in the etching solution. A potentiostat/galvanostat [Princeton Applied Research (PAR) 273] interfaced to a personal computer was used to supply the etching current. The potential transients were measured by a high speed voltmeter (Keithley 194A).

Results and Discussion

Potential transients.—Figure 1 shows the applied current waveform. t_s, the time at which the current was stepped to a lower value, was usually 5 s. i_{a2}/i_{a1}, the ratio of the final to initial applied currents, was between 0 and 0.75. Potential transients are shown in Fig. 2, at times on the order of 1 ms after current step reductions. The potential decays rapidly to a minimum after the current step. The capacitive charging current, which is proportional to the time derivative of the potential, is zero at the potential minimum; at this time, the faradaic current has adjusted to the reduced applied current. Current cycling experiments, combined with weight loss measurements, showed that the reduction of faradaic current is achieved by a decrease of metal dissolution rate from tunnel tips and not by an increased rate of cathodic hydrogen evolution.[5] For experiments in Fig. 2 where i_{a2} is larger than zero, there is an abrupt potential increase after the potential minimum, which is followed by a slower relaxation to a steady potential. The shape of the transient is somewhat different for current interruptions (where i_{a2} is zero): the potential decreases to a minimum with no undershoot, with the time of the minimum corresponding to the time of the abrupt change of slope in experiments where i_{a2} is not zero. This correspondence between the two types of potential transients is discussed more extensively below.

The contributions of surface and solution phase overpotentials to the potential transients was analyzed in prior papers.[4,5] For convenience, this analysis is summarized here. The initial potential decay can be considered as two sequential potential decreases, ΔE_1 and ΔE_2, as shown in Fig. 3, in which the transient is depicted at much longer times than in Fig. 2. ΔE_1, the difference between the initial and final steady-state potentials, is a change of the ohmic potential drop in the bulk solution due to the decreased current flow to the counterelectrode.[5] The remaining potential drop ΔE_2 is associated with individual pits or tunnels, and includes changes of the ohmic potential drop in the solution inside tunnels, as well as changes of the potential at the dissolving tunnel tip surface. $(\Delta E_2)_\Omega$, the contribution of the internal ohmic resistance to ΔE_2, was determined by measuring the variation of ΔE_2 with tunnel length.[5] It can be written as

$$(\Delta E_2)_\Omega = \left(1 - \frac{i_{a2}}{i_{a1}}\right)\frac{i_{do} v t_s}{\kappa} \qquad [1]$$

where i_{do} is the initial tunnel dissolution current density before passivation, 6.1 A/cm^2, v is the tunnel growth velocity, 2.1 μm/s, t_s is the time of the current step, and κ is the solution conductivity inside tunnels. $(\Delta E_2)_\Omega$ is 30% of ΔE_2 when t_s is 5 s (tunnel length 10.5 μm) but is insignificant compared to ΔE_2 for experiments at small step times (t_s < 0.1 s), when only cubic etch pits are present. The latter result was further supported by experiments which showed that, for passivation in cubic etch pits, ΔE_2 remained constant while the etchant solution conductivity was varied through a factor of ten.[5] According to these results, the main contribution to ΔE_2 is the variation of the potential at the surface being passivated.

Since the steady-state etching current is controlled by the ohmic resistance of the bulk solution, the potential at the metal surface under steady-state etching conditions is also the zero current intercept of the current/potential curve. This intercept is usually referred to as the repassivation, or protection potential of the metal.[1] Thus ΔE_2, when corrected for the ohmic contribution according to Eq. 1, can be identified as a surface overpotential relative to the repassivation potential.[5] Figure 4 shows that, during the initial potential decay, this surface overpotential, η_s, is linearly related to the current reduction ratio

$$\frac{i_{a2}}{i_{a1}} = \frac{i_d}{i_{do}} = 1 + k\eta_s \qquad [2]$$

where i_d is the average dissolution current density on the dissolving tip surface. k is a constant obtained from the inverse slope of Fig. 4 and is 7.94 V^{-1}. Figure 4 includes data for passivation in both tunnels and etch pits; Eq. 2 is obeyed for both structures, when the appropriate ohmic correction has been made. Since evidently η_s is the driving

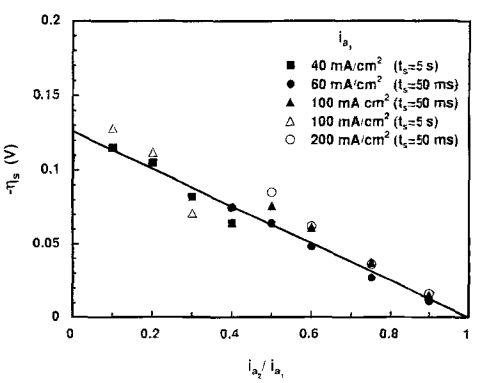

Fig. 4. Variation of surface overpotential accompanying passivation, η_s, with initial applied current density, current step time, and current reduction ratio i_{a2}/i_{a1}. The step time of 50 ms corresponds to passivation in cubic etch pits and 5 s to passivation in tunnels. In the case of tunnels, η_s was determined from ΔE_2 (Fig. 3) by correction for the internal ohmic potential drop in tunnels, according to Eq. 1. The solid line was determined by linear regression. The etchant was 1*N* HCl at 65°C.

force for repassivation, a test of any proposed passivation mechanism should be its ability to predict the potential transient. A mathematical model for the early portion of the potential transient is described in the next section.

Mathematical model.—The surface topography study[4] showed that, at times of tens of milliseconds after the current step, the tunnel tip surface was heterogeneous, consisting of 0.1 to 1 μm wide patches of actively dissolving metal surrounded by passivated surface. Patches on cubic pits were observed as early as 5 ms after the current step. When patches were present, their dissolution current density was uniform and equal to the current density at which the entire tunnel tip dissolved prior to the current step. Correspondingly, the fraction of the tip surface area occupied by the patches was equal to i_{a2}/i_{a1} (or i_d/i_{do}).

It is assumed that a surface layer, probably containing chloride ions, was present on the patch surface, and that this layer prevented passivation of the underlying metal. Before the current step, the chloride layer had covered the entire pit surface. After the step, the layer was removed from part of the surface, but remained on the patches. Removal of the chloride layer from a given point on the surface was followed by reaction of the exposed metal with water to form a passive oxide film, which effectively inhibited metal dissolution. If removal of the chloride layer was very rapid, then there was a brief time interval when the tip surface was partly covered by the chloride layer, yet no oxide film was present. The physical nature of the chloride layer is discussed further below after presentation of the model results.

In the mathematical model, the description of the surface layer was consistent with the experimental observations that (*i*) the current step caused the dissolution current in the tunnel to be reduced within about 100 μs, the time for the potential to decay to the minimum; (*ii*) this reduced dissolution current increased linearly with potential (Fig. 4 and Eq. 2); and (*iii*) at later times of a few milliseconds, dissolution was localized to small patches which corroded at a current density of i_{do}, the same as that of the entire tip surface prior to the step. To account for these observations, it was assumed that the coverage of the chloride layer on a bare metal surface depends on the potential, and responds instantly to changes in potential. Further, the dissolution current density under the chloride layer is always constant at i_{do}. The active area is related to the potential by

$$\frac{A}{A_o} = 1 + k\eta_s = 1 + k_{eff}(E - E_0) \qquad [3]$$

A/A_o is the fractional active area (or the fractional coverage of the surface layer). $(E - E_0)$, the potential drop below the steady-state potential, includes changes in both η_s and $\eta_{\Omega in}$, the ohmic overpotential inside tunnels. k_{eff} is related to k according to

$$\frac{1}{k_{eff}} = \frac{1}{k_\Omega} + \frac{1}{k} \qquad [4]$$

k_Ω is defined by $(di_{a2}/d\eta_{\Omega in})/i_{a1}$. The reciprocals of k and k_Ω are faradaic and ohmic resistances, so Eq. 4 follows from the additivity of these resistances. k_Ω was calculated from Eq. 1

$$\frac{1}{k_\Omega} = \frac{i_d v t_s}{\kappa} \qquad [5]$$

For t_s = 5 s, κ was 0.10 $(\Omega\text{-cm})^{-1}$ and k_Ω was 20.3 V^{-1}, so k_{eff} was 5.71 V^{-1}. The use of k_{eff} rather than k in Eq. 3 accounts for the effect of the ohmic potential drop in tunnels on the potential transients.

Equation 3 determines the fractional active area at every time during the initial potential decay after the current step. It was shown in the preceding paper[4] that patches are a transient feature of the corroding surface in these experiments; at potentials below E_R, they are unstable and ultimately passivate. Hence, Eq. 3 is meant to apply only during the period when oxide film formation is at an early stage, so that the chloride layer can freely configure itself. It is not valid for steady-state dissolution.

During the transient period after current reduction, the current from the aluminum electrode includes capacitive charging, metal dissolution from the tunnel tips, and current from the growth of newly formed passive film. The current balance equation may be written as

$$i_{a2} = C_d \frac{dE}{dt} + n_t A_o i_{do}[1 + k_{eff}(E - E_0)] + A_o n_t j_p(t) \qquad [6]$$

The terms on the right side of Eq. 6 are for capacitive charging, active dissolution current, and passivation current, respectively. j_p is a current density formed by dividing the passivation current by the tunnel tip area. The term for the metal dissolution current is the product of i_{do}, the uniform current density on the active part of the surface, and the total active area at a given potential, from Eq. 3. The differential capacitance, C_d, was determined from the initial decay slope of experimental potential transients, which is controlled by capacitive discharging only. The capacitance obtained in this way was 6.34 μF/cm^2, a reasonable value for oxide-covered aluminum electrodes.[6,7] Equation 6 does not include hydrogen evolution current, since this current is only 10 to 15% of the metal dissolution current,[3] and it remains constant after step changes in applied current.[5]

When the chloride layer is removed from an element of tip area, it is assumed that a characteristic decay of anodic current density on that area element is initiated. This passivation current density transient, denoted $i_p(t)$, may be ascribed to the development of an oxide film on the newly passivated surface. As an approximation, it is assumed that i_p is independent of potential, since the film growth overpotential in these experiments is about 1 V (the equilibrium potential of aluminum is −1.9 V), and this is significantly larger than the potential variation during the transients (about 50 mV, as indicated in Fig. 3). The passivation current density j_p at time t is then

$$j_p(t) = k_{eff} \int_0^t \left(-\frac{dE}{d\tau}\right) i_p(t - \tau) d\tau \qquad [7]$$

i_p is the passivation current density at a point on the tip surface. j_p at a given time is determined by the passivation currents arising from all elements of passive area which had formed prior to that time.

The characteristic passive current density transient, $i_p(t)$, was determined empirically using the potential transients for current interruption experiments, in which i_{a2} is zero. In the case of current interruptions, the entire active surface is passivated, and the potential transient is determined primarily by the capacitive charging and passivation current terms in Eq. 6. $i_p(t)$ was taken to be of the form

$$i_p = me^{-at} + ne^{-bt} \qquad [8]$$

The parameters in Eq. 8 were determined by first calculating $j_p(t)$ from the experimental potential transient for a current interruption using Eq. 6, and then using Eq. 7 and 8 to fit $j_p(t)$. The fitting procedure for the four parameters is described in detail by Tak.[8] The values of the parameters in Eq. 8 were m = −0.94 A/cm^2, n = 3.22 A/cm^2, a = 6.86 × 10^4 s^{-1}, and b = 1.85 × 10^4 s^{-1}. Figure 5 shows that the experimental $j_p(t)$ agrees closely with that calculated from Eq. 6, using these parameters. The passive current transient $i_p(t)$ obtained in this way can be used for fractional current reductions, in which i_{a2} is not zero, because it applies to a differential element of passive area, and so is not influenced by the change of total passivated area.

The passivation current density $i_p(t)$ in Eq. 8 can be used to estimate the thickness of the newly formed passive film. The film thickness is

$$\delta = \frac{\epsilon V_{ox}}{6F} \int_0^\infty i_p dt \qquad [9]$$

where V_{ox} is the molar volume of the oxide (25.5 cm^3/mol for Al_2O_3, [9] and $6F$ is the charge for formation of one mole of oxide. ε is the fractional current efficiency for film growth,

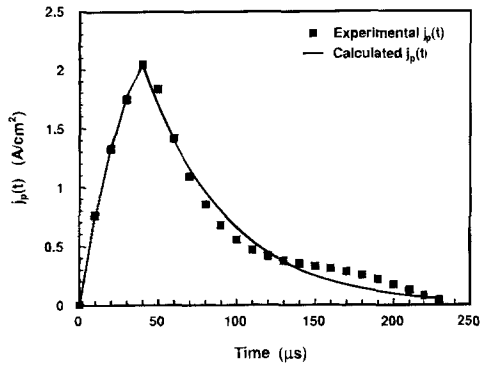

Fig. 5. Comparison of the experimental $i_p(t)$ with that calculated from Eq. 3 and 4 for a 100% current reduction. $i_p(t)$ is the faradaic current density on the passive portion of the tunnel tip surface, referred to the entire area of the tunnel tip.

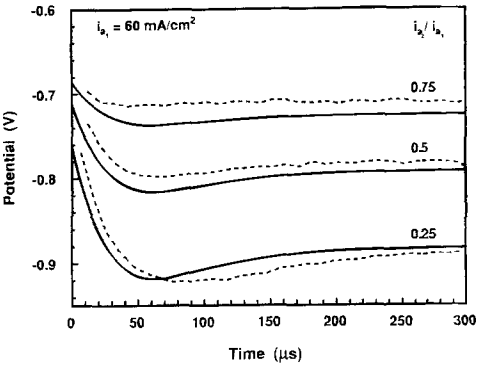

Fig. 6. Comparison of theoretical potential transients (solid lines) with measured potential transients (dashed lines) for fractional current reductions, at 65°C. Initial applied current density 60 mA/cm^2, step time 5 s. The parameter is i_{a2}/i_{a1}.

the remaining current being for dissolution of Al^{+3} ions from the film. ϵ was estimated to be 0.25 by extrapolating the film dissolution measurements of Våland and Heusler[10] at pH 0.0, to current densities in the range of 1 to 2 A/cm^2 suggested by Eq. 8. δ was calculated to be 1.2 nm. No comparable measurements of thicknesses of films formed in acidic solutions could be found. However, the electric field in aluminum oxide films is approximately constant, and the ratio of film thickness to potential drop across the film is about 1.2 nm/V.[11] Since in the present experiments film growth occurs at potentials 0.9 to 1.2 V higher than the equilibrium potential of aluminum, the film thickness should be roughly 1 nm, close to the calculated value. This thickness is somewhat smaller than that of air-formed oxide films (about 4 nm),[12] because of the significant film dissolution in acidic solutions.

The time dependence of the current in Eq. 8 can be compared to passivation current transients on bare metal surfaces, as generated for example by breaking thin metal films.[13] The time for the current to decay to $1/e$ of its initial value is about 60 μs from Eq. 8, using parameter values determined at 25°C (to be discussed below). The comparable decay times for the passivation transients measured by Frankel *et al.*[13] in a neutral solution were 10 to 25 μs. The longer decay times found here are probably caused by the relatively much lower current efficiency for film growth in acidic *vs.* neutral solutions. Since the decay time should be proportional to $1/\epsilon$, and since very little film dissolution occurs in neutral solutions, the present decay times should be about four times larger than those of Frankel *et al.*, which is in fact the case. The realistic values for both the film thickness and the passivation time found from Eq. 8 are evidence that this equation indeed represents the current during film growth on the tunnel tip surface during passivation.

Comparison of theoretical and experimental potential transients.—The predicted potential transients for current step reductions were obtained by solving the current balance equation, Eq. 6, with Eq. 7 and 8, using Laplace transforms. All parameters in these equations had been independently set by the procedures indicated above and were not variable. For times after the potential minimum, the integration in Eq. 7 was not carried through to the current time t, but was stopped at the time of the minimum. Further details of the solution procedures are given by Tak.[8] Figure 6 shows examples of experimental transients and model calculations for different current reductions when i_{a1} = 60 mA/cm^2. The results in Fig. 6 are typical of the good agreement found between theoretical and experimental transients. In particular, both experimental and predicted transients show that after the minimum at about 70 μs the potential increased by a few tens of millivolts to an approximately constant value. When the experimental transient is plotted on a larger time scale (Fig. 3), it is apparent that this "constant" potential is actually part of a relatively slow relaxation to the steady potential E_0. This slow relaxation was described in more detail in the previous paper;[4] the dominant processes during it, patch growth and passivation, are not addressed in the present model, which focuses on events during the first few hundred μs. In the following discussion, the term "potential undershoot" will be used to refer to the dip of the potential transient prior to the slow relaxation. Specifically, the undershoot is the difference between the potentials at 300 μs and at the minimum.

Figure 7 compares experimental and theoretical values for the times at the potential minimum, for experiments at 65°C, as well as at 25°C (to be discussed below). The figure shows that the predicted times at the minimum agree with experiments and that both experimental and theoretical times are controlled by the parameter $C_d/i_{a1}k$. In fact, the theoretical minimum times at 65°C are given by 3.48 $C_d/i_{a1}k$, to within 6%.

According to Eq. 6, $(i_{a1}k)^{-1}$ is the faradaic resistance of the actively dissolving aluminum surface, so this parameter is the theoretical resistance-capacitance time constant of the initial potential decay. Thus, the successful prediction of this time constant shows that the faradaic resistance of the corroding surface is well approximated by the linear variation of active area with potential in Eq. 3.

In the mathematical model, the potential undershoot is directly related to the heterogeneity of the tip surface during passivation. The potential increase after the minimum causes a recovery of the active surface area, which offsets the decrease with time of current density on the freshly

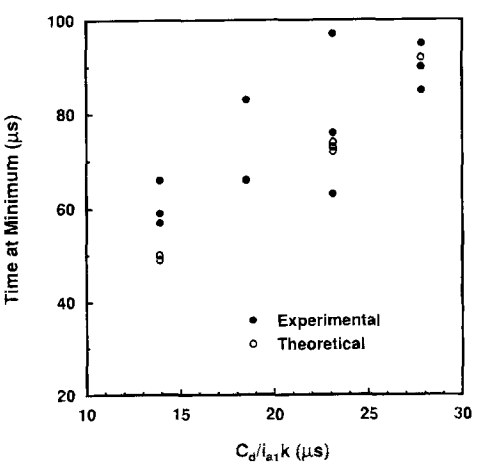

Fig. 7. Experimental and theoretically predicted times at the potential minimum, for potential transients following step reductions in applied current. Data at 65 and 25°C are both shown. For the higher temperature, the plotted points are for initial applied currents of 40, 60, and 80 mA/cm^2, and for each current, values of i_{a2}/i_{a1} of 0.25, 0.50, and 0.75. The 25°C results are those in Fig. 10.

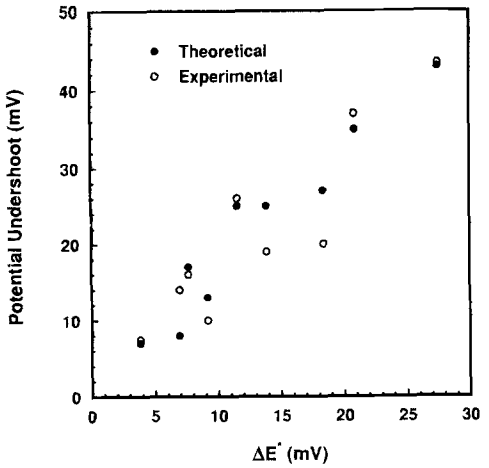

Fig. 8. Experimental and theoretically predicted potential undershoots at 65°C, as a function of the parameter ΔE^*, as defined in Eq. 10. $i_p(t_{min})$ was calculated using Eq. 8 for i_p, and t_{min} is 3.48 $C_d/i_{a1}k$, as discussed in the test. Plotted points are for initial applied currents of 40, 60, and 80 mA/cm^2, and, for each current, values of 0.25, 0.50, and 0.75 for i_{a2}/i_{a1}.

passivated surface (Eq. 8). According to these concepts, the potential undershoot can be roughly estimated as ΔE^*, defined by

$$\Delta E^* = \frac{\left(1 - \frac{i_{a2}}{i_{a1}}\right) i_p(t_{min})}{i_{do}k} \qquad [10]$$

In this expression, $(1 - i_{a2}/i_{a1})$ represents the fraction of the tip area which passivates, and t_{min} is 3.48 $C_d/i_{a1}k$, as given above, the approximate time of the potential minimum. Since the final passive current density is zero (Eq. 8), $i_p(t_{min})$ represents the total decrease of passive current density after the potential minimum. Hence, the numerator in Eq. 10 is the decrease of passive current after the minimum. As in the model itself, it is assumed in Eq. 10 that the compensating increase of active area follows Eq. 3, and is $k\Delta E^*$. The corresponding increase of dissolution current after the minimum is $i_{do}k\Delta E^*$. Equation 10 approximates the potential undershoot in the model, but is not exact because it does not account for capacitive charging current, nor the variable age of the passive film at different points on the surface. Comparison of Fig. 5 and 6 indicates that the increase of active area during the undershoot occurs after most of the tip surface is already occupied by passive film. Thus, the active area increase may involve reversible desorption of oxide ions from parts of the surface on which passive film growth had just initiated.

Figure 8 shows the experimental and predicted potential undershoots at 65°C, for various current reductions and initial applied currents, plotted *vs.* ΔE^*. Two important results may be drawn from the figure. First, the theoretical undershoot is indeed controlled by ΔE^*, as was argued above. Also, experimental and theoretical undershoots are in good mutual agreement. The main factor accountng for the variability of ΔE^* in Fig. 8 is $(1 - i_{a2}/i_{a1})$, which determines the extent of oxide film coverage on the tip surface. In addition to the film coverage, the undershoot also depends on the passivation current decay, the dissolution current density, and the variation of the active area with potential. Thus, the undershoot tests a number of important features of the model. The good quality of this prediction is evidence that all these factors have been depicted realistically.

In summary, the model calculations compare favorably with experiment, particularly with regard to the time of the minimum potential and the potential undershoot. Also, the passivation current transient derived from the model gives a reasonable film thickness and decay time. The success of these predictions supports the central assumption of the model, which is the rapid variation of active area with potential according to Eq. 3. Partial coverage with passive surface, which was observed microscopically at times at least 5 ms after current steps, evidently occurs within tens of microseconds after the step.

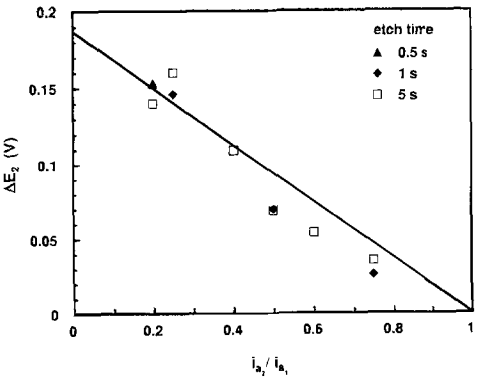

Fig. 9. Variation of potential drop ΔE_2 with i_{a2}/i_{a1} at 25°C, for different current step times. The etchant was 1*N* HCl and i_{a1} was 40 mA/cm^2.

When aluminum is etched at constant applied current in 1*N* HCl at 25°C, no tunnels are observed, but only corrosion pits having crystallographic facets but irregular overall shapes. The model was used to predict potential transients following current step reductions, for experiments under these conditions. In this way, it was investigated whether the model might apply with some generality to localized corrosion of aluminum, or would instead be specifically valid only for aluminum etch tunnels. The model parameters at ambient temperature were obtained in the same way as at 65°C. Figure 9 shows that the potential drop ΔE_2 is related linearly to the current reduction ratio, similar to Fig. 4 for the higher temperature. The parameters for ambient temperature were: $C_d = 4.92$ μF/cm^2, $k_{eff} = 5.33$ V^{-1}, $m = -0.99$ A/cm^2, $n = 3.75$ A/cm^2, $a = 8.7 \times 10^4$ s^{-1}, and $b = 2.1 \times 10^4$ s^{-1}. The experimental and theoretical potential transients after current reductions are similar to those at 65°C, as shown in Fig. 10. As at the higher temperature, the predictions of the model follow the experimental potential transients closely. This agreement suggests that the uniqueness of the geometry of aluminum etch tunnels is not related to features of the passivation mechanism which are specific to the growth form. In other words, the overall shape of the localized corrosion cavity appears not to be coupled to the passivation mechanism.

Discussion of the mechanism of passivation.—As discussed above, the active area is believed to be defined by the presence of a chloride containing surface layer whose coverage depends on potential. This layer would have the required feature of potential-dependent coverage if it simply consists of specifically adsorbed chloride ions. Since

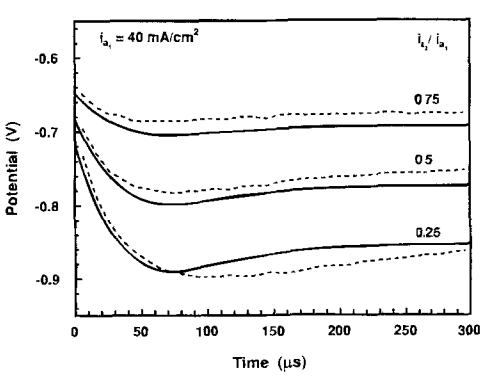

Fig. 10. Comparison of theoretical potential transients (lines) with measured potential transients (markers) for fractional current reductions, at 25°C. Initial applied current density 40 mA/cm^2, step time 5 s. The parameter is i_{a2}/i_{a1}.

the configuration of the surface layer is determined during the first tens of microseconds after the current step, when the surface is relatively free of oxide film, its features would probably be similar to those of halide ion adsorption layers on unfilmed metal electrodes (*i.e.*, noble metals and mercury). Chloride ions specifically adsorb on most of these surfaces; their coverage is in general zero near the potential of zero charge (E_{pzc}), and increases monotonically as a function of potential (in many cases, approximately linearly) above E_{pzc}.[14] On corroding aluminum surfaces, the potential of unit coverage would be the repassivation potential E_R, since at this potential surfaces in pits dissolve uniformly ($A/A_o = 1$). According to Delahay, the kinetics of adsorption (at least on mercury electrodes) are very rapid, and the adsorption or desorption rate is usually determined by other rate processes in series with adsorption.[15] In this case, the layer of adsorbed chloride ions would also have the required feature of rapid response of surface coverage to changes in the potential.

If this adsorption model is correct, the potential for zero fractional active area, according to Eq. 3, should be the same as the potential of zero charge of aluminum, where the surface concentration of adsorbed chloride ions would be zero. E_{pzc} of aluminum has not been measured directly, because the surface oxide film is always present when the metal is in contact with aqueous solutions. However, on the basis of the correlation between work functions and the potentials of zero charge, Trassati[16] estimated the E_{pzc} for aluminum at 25°C to be −0.84 V *vs.* the normal hydrogen electrode, or −1.03 V *vs.* the Ag/AgCl reference electrode. This correlation is obeyed for other metals to within 50 to 100 mV. Therefore, within the accuracy of Trassati's correlation, the potential of zero charge agrees with potential (−0.93 V *vs.* Ag/AgCl) at which the active area at 25°C becomes zero according to Eq. 3.

As the potential is decreased from the repassivation potential, E_R, to E_{pzc}, a range of 126 mV, the chloride surface coverage should decrease from unity to zero. Interestingly, Valette and Parsons[17] found that the surface coverage of specifically adsorbed chloride ions on silver (110) surfaces increased from 0 to 1 over a closely comparable potential range of 120 mV above E_{pzc}. The variation of chloride surface concentration with potential in this range was approximately linear, as also suggested by Eq. 3. It is not known how general this behavior should be for various metals. It should also be mentioned that close-packed adsorbate islands are a common observation on metal surfaces.[18] Indeed, evidence for bromide islands on silver in electrochemical environments has been presented.[19] These adsorbate islands could be the origin of the localized patches of metal dissolution observed here.

This adsorption model for corroding surfaces in pits is similar in some ways to previous speculations by Kolotyrkin[20] and by Leckie and Uhlig.[21] These investigators each attributed critical potentials for pitting to potential-dependent adsorption of aggressive anions. However, both Kolotyrkin and Uhlig viewed adsorption as reversible, in the sense that the anions could directly displace oxide from the surface. In contrast, the present model suggests that reversible anion adsorption occurs only at very early times during passivation, when the oxide film has not yet fully formed. Once the oxide film is present, Eq. 3 no longer determines the anion coverage. This is effectively demonstrated by the topographic observations in the preceding paper,[4] which showed that, as the potential increased from its minimum value to E_R, the active area did not increase but remained constant.

Conclusions

The initial moments of oxide film passivation of corroding aluminum surface in etch tunnels and pits were investigated. Passivation was initiated by step reductions in the applied current. A mathematical model of potential transients during passivation was developed; the predictions of the model were compared to experimental transients measured at times less than 1 ms after the initiation of passivation. The model assumes that, at these times, the corroding surface is microscopically heterogeneous, consisting of separated active and passive areas. The instantaneous distribution of passive and active areas is determined by the electrode potential: the fractional active area increases linearly with potential and is unity at the repassivation potential. This view of a potential dependent distribution of active and passive areas is consistent with microscopic observations of the evolution of surface topography during passivation.[4]

The theoretical transients showed a potential undershoot at a time of about 0.1 ms; both the time and extent of this undershoot were in quantitative agreement with experiment. It was shown that the undershoot is directly related to the formation of microscopic passive areas on the corroding surface at these times. Thus, this detailed agreement between theory and experiment is evidence for the main premise of the model, which is that the fractional coverage of active area adjusts nearly instantaneously to changes in the potential.

The present observations of the initial stages of passivation are consistent with a model in which the corroding surface is occupied by a layer of specifically adsorbed chloride ions. Oxide film coverage is initiated by desorption of these ions. The reconfiguration of the surface layer occurs during a time which is small enough (tens of microseconds), so that the extent of oxide film formation is still small.

Acknowledgments

Aluminum foil samples were provided by KDK Corporation, Takahagi, Japan.

Manuscript submitted June 3, 1993; revised manuscript received Jan. 11, 1994.

LIST OF SYMBOLS

A	active area on tunnel tip, cm^2
A_0	tunnel tip area, cm^2
a, b	empirical constants in passivation current density, s^{-1}
C_d	electrode surface capacitance, F/cm^2
E	measured potential corrected for bulk solution ohmic potential drop, V
E_0	steady-state potential corrected for bulk solution ohmic potential drop, V; (also repassivation potential at bulk solution composition)
E_R	empirical repassivation potential of aluminum, V
F	Faraday constant, 96,487 C/equiv
i_{a1}	applied current density prior to current step, A/cm^2 (applied current/electrode area)
i_{a2}	applied current density after curent step, A/cm^2 (applied current/electrode area)
i_d	dissolution current density, A/cm^2 (dissolution current/tip area)
i_{do}	dissolution current density, A/cm^2 (dissolution current/active area)
i_p	passive current density on tunnel tip, A/cm^2 (passive current/passive area)
j_p	passive current density on tunnel tip, A/cm^2 (passive current/tip area)
k	empirical constant relating fractional active area to potential, V^{-1}
k_{eff}	modified k to account for ohmic resistance of tunnel, V^{-1}
k_Ω	constant representing ohmic conductance of tunnel, V^{-1}
m, n	empirical constants in passivation current density, A/cm^2
n_t	number of tunnels per unit electrode area, cm^{-2}
t	difference between current time and time of current step, s
t_{min}	difference between time of potential minimum and time of current step, s
t_s	difference between time of current step and time when current initially applied, s
V_{ox}	molar volume of aluminum oxide in the passive film, cm^3/mol
v	dissolution velocity, cm/s
ΔE_1	difference between steady-state potentials before and after current step, V
ΔE_2	difference between steady-state potential after current step and potential minimum, V
$(\Delta E_2)_\Omega$	contribution of tunnel ohmic potential drop to ΔE_2, V

ΔE^* parameter giving estimate of potential undershoot, V
ϵ fractional current efficiency for film growth
δ passive film thickness, cm
η_s surface overpotential, V (potential at dissolving surface minus repassivation potential at solution composition adjacent to surface)
$\eta_{\Omega m}$ ohmic overpotential inside tunnels, V
κ solution conductivity inside tunnels, $(\Omega\text{-cm})^{-1}$
τ variable of integration, s

REFERENCES

1. Z. Sklarska-Smialskowska, *Pitting Corrosion of Metals*, NACE, Houston (1986).
2. R. S. Alwitt, T. R. Beck, and K. R. Hebert, in *Advances in Localized Corrosion*, H. S. Isaacs, Editor, p. 145, NACE, Houston, TX (1990).
3. R. S. Alwitt, H. Uchi, T. R. Beck, and R. C. Alkire, *This Journal*, **131,** 13 (1984).
4. Y. Tak, E. R. Henderson, and K. R. Hebert, *ibid.*, **141,** 1446 (1994).
5. B. J. Wiersma, Y. Tak, and K. R. Hebert, *ibid.*, **138,** 371 (1991).
6. B. J. Wiersma and K. R. Hebert, *ibid.*, **138,** 48 (1991).
7. W. Wilhelmsen and T. Hurlen, *Electrochim. Acta*, **32,** 95 (1987).
8. Y. Tak, Ph.D. Thesis, Iowa State University, Ames, Iowa (1993).
9. *Handbook of Chemistry and Physics*, 51st ed., R. C. Weast, Editor, p. B-64, The Chemical Rubber Co., Cleveland, OH (1970).
10. T. Våland and K. E. Heusler, *J. Electroanal. Chem.*, **149,** 71 (1983).
11. W. J. Bernard and J. W. Cook, *This Journal*, **106,** 643 (1959).
12. P. B. Barna, Z. Bodó, G. Gergely, P. Croce, J. Ádám, and P. Jakab, *Thin Solid Films*, **43,** 303 (1977).
13. G. S. Frankel, B. M. Rush, C. V. Jahnes, C. E. Farrell, A. J. Davenport, and H. S. Isaacs, *This Journal*, **138,** 643 (1991).
14. M. A. Habib and J. O'M. Bockris, in *Comprehensive Treatise on Electrochemistry*, Vol. 1, J. O'M. Bockris, B. E. Conway, and E. Yeager, Editors, p. 135, Plenum Press, New York (1980).
15. P. Delahay, *Double Layer and Electrode Kinetics*, p. 118, Interscience Publishers, New York (1965).
16. S. Trasatti, in *Advances in Electrochemistry and Electrochemical Engineering*, Vol. 10, H. Gerischer and C. W. Tobias, Editors, p. 259, Wiley, New York (1977).
17. G. Valette and R. Parsons, *J. Electroanal. Chem.*, **204,** 291 (1986).
18. M. G. Lagally, G.-C. Wang, and T.-M. Lu, in *Chemistry and Physics of Solid Surfaces*, Vol. II, R. Vanselow, Editor, p. 153, CRC Press, Boca Raton, FL (1979).
19. K. Bange, B. Straehler, J. K. Sass, and R. Parsons, *J. Electroanal. Chem.*, **229,** 87 (1987).
20. Ja. M. Kolotyrkin, *This Journal*, **108,** 209 (1961).
21. H. P. Leckie and H. H. Uhlig, *ibid.*, **113,** 1262 (1966).